UC Davis

UC Davis Previously Published Works

Title

Identification of a metabolic disposal route for the oncometabolite S-(2-succino)cysteine in Bacillus subtilis

Permalink

https://escholarship.org/uc/item/50c7p29f

Journal

Journal of Biological Chemistry, 293(21)

ISSN

0021-9258

Authors

Niehaus, Thomas D
Folz, Jacob
McCarty, Donald R
et al.

Publication Date

2018-05-01

DOI

10.1074/jbc.ra118.002925

Peer reviewed

eScholarship.org Powered by the California Digital Library
University of California

Identification of a metabolic disposal route for the oncometabolite *S*-(2-succino)cysteine in *Bacillus subtilis*

Received for publication, March 14, 2018, and in revised form, April 4, 2018 Published, Papers in Press, April 6, 2018, DOI 10.1074/jbc.RA118.002925

Thomas D. Niehaus[‡1], Jacob Folz[§], Donald R. McCarty[‡], Arthur J. L. Cooper[¶], David Moraga Amador[‖], Oliver Fiehn[§], and Andrew D. Hanson[‡2]

From the [‡]Horticultural Sciences Department and [‖]Interdisciplinary Center for Biotechnology Research, University of Florida, Gainesville, Florida 32611, the [§]West Coast Metabolomics Center, University of California, Davis, California 95616, and the [¶]Department of Biochemistry and Molecular Biology, New York Medical College, Valhalla, New York 10595

Edited by Ursula Jakob

Cellular thiols such as cysteine spontaneously and readily react with the respiratory intermediate fumarate, resulting in the formation of stable *S*-(2-succino)-adducts. Fumarate-mediated succination of thiols increases in certain tumors and in response to glucotoxicity associated with diabetes. Therefore, *S*-(2-succino)-adducts such as *S*-(2-succino)cysteine (2SC) are considered oncometabolites and biomarkers for human disease. No disposal routes for *S*-(2-succino)-compounds have been reported prior to this study. Here, we show that *Bacillus subtilis* metabolizes 2SC to cysteine using a pathway encoded by the *yxe* operon. The first step is *N*-acetylation of 2SC followed by an oxygenation that we propose results in the release of oxaloacetate and *N*-acetylcysteine, which is deacetylated to give cysteine. Knockouts of the genes predicted to mediate each step in the pathway lose the ability to grow on 2SC as the sulfur source and accumulate the expected upstream metabolite(s). We further show that *N*-acetylation of 2SC relieves toxicity. This is the first demonstration of a metabolic disposal route for any *S*-(2-succino)-compound, paving the way toward the identification of corresponding pathways in other species.

The respiratory intermediate fumarate, an electrophilic α,β-unsaturated dicarboxylate, reacts spontaneously and readily with soft nucleophiles such as sulfhydryl groups in a process known as succination (1, 2). Fumarate and the sulfhydryl group of cysteine undergo succination to form the stable compound *S*-(2-succino)cysteine (2SC),[3] which exists as two diastereomers due to the chirality of the *S*-(2-succino) bond; this reaction can occur with free cysteine as well as with cysteinyl residues of proteins and small-molecule thiols such as GSH (1, 2) (Fig. 1). Succination of proteins and GSH is biologically significant due to their high cellular concentrations and because their cysteinyl residues can be significantly more acidic (and hence nucleophilic) than free cysteine (1, 2). Cysteine residues located in enzyme active sites are likely to exist as strongly nucleophilic thiolate anions (3), making thiol enzymes particularly prone to succination (4). Several proteins with functional cysteine residues are known to be susceptible to succination that results in impaired functionality, including glyceraldehyde-3-phosphate dehydrogenase (5, 6), aconitase (7), actin and tubulin (8, 9), and chaperone proteins (9). At least 182 succinated proteins have been detected in humans (10). Succination is thus a common and well-described post-translational chemical modification of proteins.

The degree of succination of biological thiols is directly related to fumarate concentration (1). Accordingly, 2SC can serve as a biomarker for abnormalities in aerobic respiration that cause fumarate buildup. In humans, germline mutations that inactivate the citric acid cycle enzyme fumarate hydratase cause fumarate accumulation and increase the succination of cellular thiols; such mutations predispose to hereditary leiomyomatosis and renal cell cancer syndrome (11–13). 2SC is considered an oncometabolite because of its accumulation in certain cancers (14). An increase in succination due to fumarate accumulation is also observed in adipose tissue under the hyperglycemic conditions associated with type 2 diabetes and obesity (15–17). Succination of proteins has many deleterious effects (18–21). Additionally, succination of GSH can lead to persistent oxidative stress and cellular senescence (22). The harmful effects of succination suggest that this process is more than just a symptom of mitochondrial stress or dysfunction in chronic diseases but that succination actually contributes to the pathogenesis of disease complications. In support of this, recent studies suggest that succination is the mechanistic link between mitochondrial and endoplasmic reticulum complications in diabetes (23).

Much research has focused on targets of succination and the role of succination in disease but not on the metabolism of 2SC after it forms. No metabolic disposal route for 2SC has yet been demonstrated. Here, we present biochemical and genetic analyses showing that *Bacillus subtilis* has a breakdown pathway that is specific for 2SC. These analyses implicate the *yxe* operon in 2SC breakdown, show that the pathway begins with acetylation and ends with deacetylation, and confirm that 2SC is toxic.

This work was supported by National Science Foundation Grant MCB-1153413 and by an endowment from the C. V. Griffin Sr. Foundation. The authors declare that they have no conflicts of interest with the contents of this article.

This article contains Figs. S1–S5 and Tables S1 and S2.

[1] To whom correspondence may be addressed: Horticultural Sciences Dept., University of Florida, 1301 Fifield Hall, 2550 Hull Rd., Gainesville, FL 32611. Tel.: 352-273-4856; Fax: 352-392-5653; E-mail: tomniehaus@ufl.edu.

[2] To whom correspondence may be addressed: Horticultural Sciences Dept., University of Florida, 1301 Fifield Hall, 2550 Hull Rd., Gainesville, FL 32611. Tel.: 352-273-4856; Fax: 352-392-5653; E-mail: adha@ufl.edu.

[3] The abbreviations used are: 2SC, *S*-(2-succino)cysteine; NAC, *N*-acetyl-L-cysteine; Tn-seq, transposon sequencing.

© 2018 Niehaus et al. Published under exclusive license by The American Society for Biochemistry and Molecular Biology, Inc.

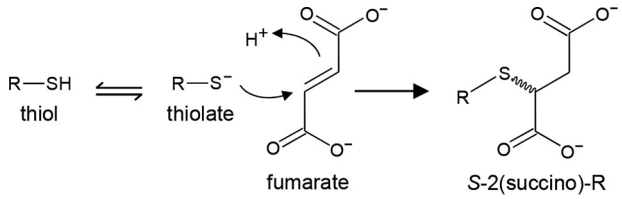

Figure 1. Spontaneous reaction of fumarate with thiols. Succination occurs when thiols (or more specifically, thiolate ions) of cysteine, cysteinyl residues, GSH, or other compounds react with fumarate to form stable *S*-(2-succino)-derivatives.

Results

B. subtilis uses 2SC as a sulfur source

We first tested whether *Escherichia coli* or *B. subtilis* can utilize 2SC as the sulfur source. 2SC served as an excellent sulfur source for *B. subtilis* but not *E. coli* (Fig. S1). A cysteine auxotroph of *B. subtilis* (Δ*yrhA* Δ*cysK*) (24) also grew well on 2SC (Fig. S2), demonstrating that *B. subtilis* can metabolize 2SC to cysteine.

A high-throughput screen implicates the yxe operon in 2SC utilization

To identify the gene(s) required to metabolize 2SC, we used a high-throughput screen with a *B. subtilis* library containing ~7.3×10^4 unique *magellan6x* transposon insertions (*i.e.* Tn-seq) (25). The initial transposon-mutant population was grown for six generations on defined medium containing 2SC, sulfate, or methionine as the sulfur source. Afterward, the transposon insertion sites were sequenced, allowing us to map the location and relative frequency of each transposon insertion for each experiment. If a gene is important for growth on one particular sulfur source, then the relative frequency of transposon insertions located within that gene will decrease in the population grown on that sulfur source relative to the others. Different transposon insertions can result in varying degrees of gene silencing, so a gene may still contain transposons even if it is essential under a certain growth condition.

Sulfate- or methionine-grown populations served as both controls and comparisons for the 2SC-grown population. As expected, nearly every gene involved in cysteine and methionine synthesis was essential when grown on sulfate but not when grown on methionine (Fig. S3). Because *B. subtilis* can metabolize 2SC to cysteine (Fig. S2), growing cells on 2SC is functionally equivalent to growing cells on cysteine. Accordingly, genes involved in the conversion of cysteine to methionine were essential when grown on 2SC (Fig. S3). Observing the expected trends in the different sulfur-source populations validated the screening procedure. The only genes that significantly affected fitness in the 2SC-grown population but not in either sulfate- or methionine-grown populations were genes of the *yxe* operon (Fig. 2), particularly *yxeK* and *yxeL*.

The yxe operon and its distribution

The *yxe* operon consists of seven genes that encode a predicted FAD-dependent monooxygenase, *yxeK*; an acetyltransferase, *yxeL*; three components of an ATP-transporter complex, *yxeMNO*; an *N*-acetylcysteine deacetylase, *yxeP*; and a putative dehydratase, *yxeQ*. No specific role for the *yxe* operon has been ascribed, but there is evidence that the acetyltransferase *yxeL* and *N*-acetylcysteine deacetylase *yxeP* may participate in the degradation of *S*-methylcysteine, and they have been named *snaB* and *sndB*, respectively (26). Here, we retain *yxe* designations. The *yxe* operon is widely distributed in bacteria, occurring in firmicutes and α-, β-, and γ-proteobacteria (Fig. S4). *E. coli* lacks both the *yxe* operon and the ability to use 2SC as a sulfur source (Fig. S2). *A priori*, it is reasonable to predict that the *yxe* operon plays a role in 2SC metabolism.

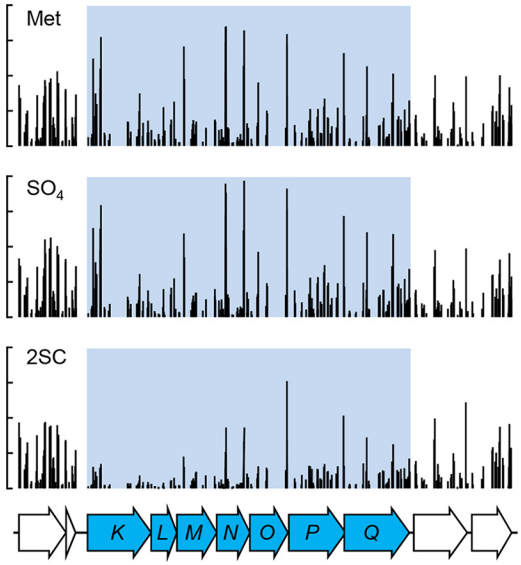

Figure 2. Tn-seq indicates that the *yxeKLMNOPQ* operon is important for SSC breakdown in *B. subtilis*. Tn-seq was performed on a library of random transposon insertion mutations in *B. subtilis* grown for six doublings in defined medium containing either 2 mM sulfate (SO_4), 1 mM L-methionine (*Met*), or 1 mM 2SC as the sole sulfur source. Each histogram shows the location and relative frequency of transposon insertions in the indicated genome region. The *yxeKLMNOPQ* operon is colored *blue* in the gene model and shaded *blue* in the histograms. Data for the two genes flanking each side of the *yxeKLMNOPQ* operon (uncolored in the gene model and histograms) are shown for comparison.

Analysis of mutants confirms a role for yxe genes in 2SC metabolism

Because Tn-seq indicated that *yxe* operon genes play a role in 2SC metabolism, we obtained a BKE knockout mutant (27) for each of the *yxe* operon genes and tested the mutants' ability to grow on 2SC as the only sulfur source. Deletants of the monooxygenase *yxeK* and the acetyltransferase *yxeL* were severely limited in their ability to grow on 2SC with only a slight trace of growth observed for either mutant (Fig. 3*A*). In contrast, no obvious growth defect was observed for the other *yxe* gene deletants (Fig. 3*A*).

The acetyltransferase YxeL has a homolog in *B. subtilis*, SnaA, that is reported to acetylate certain *S*-alkylcysteine adducts such as *S*-methylcysteine (26). An *snaA* deletant grew well on 2SC; however, a mutant lacking both acetyltransferase genes *yxeL* and *snaA* showed no sign of growth on 2SC (Fig. 3*B*), indicating that an acetylation step is critical for 2SC metabolism and that *snaA* can partially compensate for *yxeL* deficiency. Besides *yxeP*, *B. subtilis* has two other functionally redundant *N*-acetylcysteine deacetylase genes, *sndA* and *sndC* (26). As was observed for the *yxeP* deletant, mutants of *sndA* and *sndC* grew

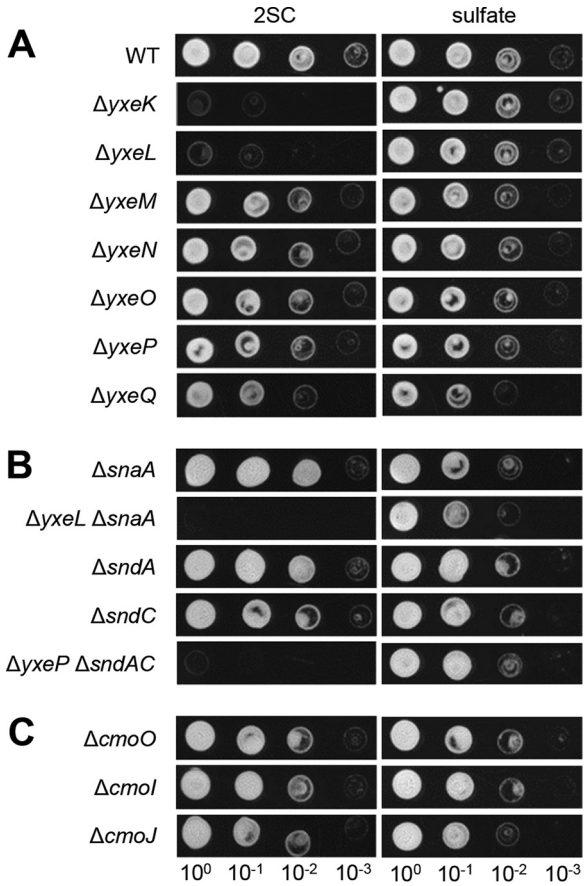

Figure 3. Growth of various *B. subtilis* mutants on 2SC. WT *B. subtilis* and *yxe* operon gene knockouts (*A*), various acetyltransferase and deacetylase mutants (*B*), and various monooxygenase mutants (*C*) were grown overnight in LB medium with the appropriate antibiotic; washed twice with water; and diluted to optical density 10^0, 10^{-1}, 10^{-2}, and 10^{-3}, and 10 μl was spotted on medium with either 1 mM 2SC or 2 mM sulfate as the sulfur source. Incubation was for 16 h at 37 °C.

well on 2SC. However, a mutant lacking all three deacetylase genes did not grow on 2SC (Fig. 3*B*). These results suggest that a pathway to metabolize 2SC to cysteine involves acetylation and deacetylation steps, similar to a proposed pathway for the degradation of other *S*-alkylcysteine adducts (26).

Three monooxygenase genes, *cmoO*, *cmoI*, and *cmoJ*, have all been reported to be essential for the degradation of *S*-methylcysteine and other *S*-alkylcysteine adducts (26). Mutants of each of these genes grew well on 2SC (Fig. 3*C*), indicating that, apart from the acetylation and deacetylation steps, the breakdown of 2SC requires distinct genes from that of *S*-methylcysteine.

YxeL is a highly efficient 2SC N-acetyltransferase

Tn-seq and growth experiments indicate that the acetyltransferase gene *yxeL* is important for 2SC metabolism, but growth tests show that *snaA* may partially compensate for *yxeL*. To test their relative ability to acetylate 2SC, we purified heterologously expressed YxeL and SnaA proteins and assayed their 2SC *N*-acetyltransferase activity. YxeL could acetylate essentially all the 2SC present in the assay mixture, indicating that it acts on both diastereomers of 2SC, which should be present in equimolar amounts (1, 2). The K_m for YxeL is in the low micromolar range, which is more than 50-fold lower than that for SnaA (Table 1). The turnover number for YxeL is more than 250-fold higher than that for SnaA, making YxeL about 13,000-fold more catalytically efficient (Table 1). This fits with the Tn-seq and growth data that indicate that *yxeL* is far more important than *snaA* for 2SC metabolism. These kinetic parameters are consistent with 2SC being a physiological substrate for YxeL.

Table 1
Kinetic properties of recombinant YxeL and SnaA proteins
Activities were determined at 37 °C as described under "Experimental procedures." Values are means and S.E. of three replicates.

Protein	K_m	K_{cat}	K_{cat}/K_m
	μM	s^{-1}	$mM^{-1}\cdot s^{-1}$
YxeL	86.4 ± 1.6	9.5 ± 0.6	110
SnaA	4380 ± 240	0.037 ± 0.001	0.0084

YxeL alleviates 2SC toxicity in B. subtilis by N-acetylation

YxeL is a highly efficient 2SC *N*-acetyltransferase and catalyzes a critical step in 2SC metabolism. Acetylation of toxic or unwanted compounds is a common strategy used by bacteria (28), raising the possibility that YxeL alleviates 2SC toxicity. To assess this, we tested whether 2SC inhibits growth of a *B. subtilis yxeL* mutant. Wildtype (WT) or *yxeL* deletant cells were overlaid on a plate containing sulfate as the sulfur source, and 2SC was added to the center of the plate. 2SC caused a zone of growth inhibition to occur on *yxeL* deletant but not WT *B. subtilis*, whereas *N*-acetyl-*S*-(2-succino)cysteine (*N*-acetyl-2SC) did not inhibit growth of either strain (Fig. 4). These data indicate that 2SC is a toxic compound, at least in *B. subtilis* at high exogenous concentrations, and that *N*-acetylation relieves toxicity.

Metabolite profiling confirms a breakdown pathway

Our data indicate that the first step in 2SC breakdown is *N*-acetylation and that oxygenation and deacetylation steps are also required. A reasonable scenario involves acetylation of 2SC followed by oxygenation of *N*-acetyl-2SC and formation of *N*-acetylcysteine (NAC), which is deacetylated to give cysteine, analogous to the proposed breakdown pathway of other *S*-alkylcysteine compounds (26). If this proposed pathway for 2SC deconstruction is correct, then mutants should accumulate their respective upstream pathway intermediates.

The first step in the pathway is acetylation of 2SC. Thus, we predicted that acetyltransferase (*e.g. yxeL*) mutants would accumulate 2SC. We profiled *B. subtilis* cells grown on medium containing fumarate as the carbon source in an attempt to increase the spontaneous succination of thiols by fumarate, thereby increasing 2SC formation. 2SC was detected in both WT and *snaA* deletant cells, but *yxeL* deletants accumulated around 70-fold more 2SC (Fig. 5*A*). There was no significant difference in 2SC levels between the *yxeL* deletant and *yxeL snaA* double mutant cells (Fig. 5*A*). These data confirm that the *yxeL* gene product is the main enzyme controlling 2SC levels *in vivo*.

We proposed that YxeK is a monooxygenase that acts on *N*-acetyl-2SC. Thus, *yxeK* mutants should accumulate *N*-acetyl-2SC. We profiled *B. subtilis* cells grown on medium

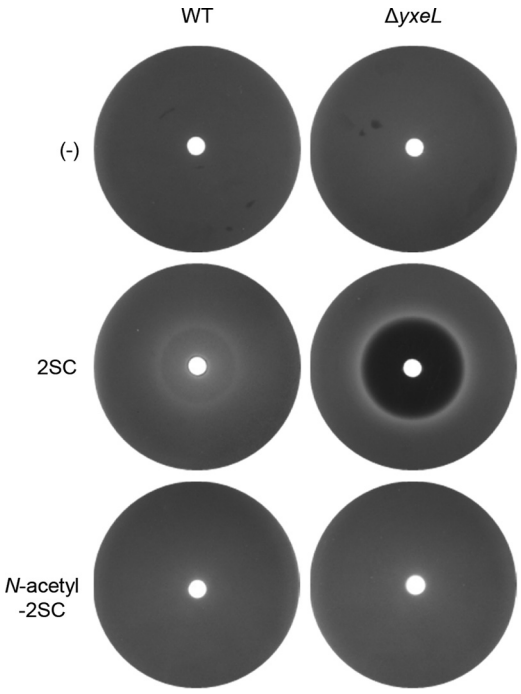

Figure 4. 2SC is toxic to *B. subtilis* unless it is *N*-acetylated. Plates containing medium with 100 μM sulfate as the sulfur source were overlaid with WT or Δ*yxeL B. subtilis* cells, and a Whatman paper disc containing water (−) or 10 μmol of the indicated compound was placed in the center of the plate. Pictures were taken after 24-h incubation at 37 °C and are representative of four independent experiments.

containing glucose as the carbon source but were unable to detect *N*-acetyl-2SC in WT or *yxeK* deletant cells (Fig. 5*B*). In an attempt to force carbon flux through the 2SC breakdown pathway, we added 2SC to the culture either 10 or 60 min prior to harvesting the cells. When 2SC was added to the culture 10 min prior to harvesting, *yxeK* deletant cells showed a massive accumulation of *N*-acetyl-2SC to around 8 μmol mg^{-1} of protein (Fig. 5*B*). By 60 min after 2SC addition, *N*-acetyl-2SC was still readily detectable, but the levels decreased about 25-fold compared with 10 min after 2SC addition (Fig. 5*B*). There was also a small but significant increase in NAC at 60 min after 2SC addition (Fig. 5*B*). These data indicate that the *yxeK* gene product plays a major role in the breakdown of 2SC by acting on *N*-acetyl-2SC, likely giving rise to NAC. Because the levels of *N*-acetyl-2SC decreased and NAC slightly increased between 10 and 60 min after 2SC addition to the mutant, there may be one or more functionally redundant mechanisms that can partially compensate for the loss of YxeK.

YxeP is predicted to be an NAC deacetylase that completes the 2SC breakdown pathway. Because growth tests indicated that *B. subtilis* has three functionally redundant NAC deacetylase genes (Fig. 3*B*), we profiled the triple mutant strain (Δ*yxeP* Δ*sndAC*). Cells were grown in the same manner as the *yxeK* deletants. There was no increase in NAC 10 min after addition of 2SC, but there was a significant increase in *N*-acetyl-2SC (Fig. 5*C*). At 60 min after 2SC addition, NAC levels increased about 60-fold, and *N*-acetyl-2SC levels increased about 10-fold compared with the values obtained at 10 min after 2SC addition (Fig. 5*C*). These data show that the levels of both upstream intermediates, *N*-acetyl-2SC and NAC, increase in the NAC deacetylase triple mutant and provide evidence in support of the proposed pathway.

Discussion

Our results provide strong biochemical and genetic evidence that genes of the *yxe* operon are primarily responsible for 2SC breakdown in *B. subtilis*. The initial breakdown step is *N*-acetylation of 2SC, a reaction that YxeL performs remarkably well (Table 1). The catalytic efficiency (K_{cat}/K_m) of YxeL is ~350-fold higher than that of bacterial serine acetyltransferase, which is another small-molecule acetyltransferase involved in cysteine metabolism (29). This high efficiency might be necessary because of the toxicity of 2SC (Fig. 4) and thus the need to avoid its accumulation. Our data show that the concentration of 2SC is maintained below 5 μM in *B. subtilis* cells (assuming a cell volume of 4.6 fl (30)) unless *yxeL* is disrupted, even when grown under conditions that should favor an increase in succination (Fig. 5*A*). In addition to initiating the salvage of cysteine from 2SC, YxeL may also prevent the accumulation of a toxic metabolite by converting it to a more benign form. If that were the case, then *yxeL* would fit the definition of a metabolite damage-preemption gene (31).

The next step in 2SC breakdown, carried out by YxeK, is likely oxygenation of the succinyl moiety of *N*-acetyl-2SC, leading to the release of NAC. One possible mechanism for this step is that YxeK hydroxylates the 2-position of the succinyl moiety of *N*-acetyl-2SC, causing a spontaneous elimination reaction of the resulting hemithioketal that generates oxaloacetate and NAC (Fig. 5*D*). Although other mechanisms are formally possible, the intermediate described above is analogous to the hemithioacetal intermediate of the glyoxalase I reaction that is formed from the reversible reaction of methyglyoxal with GSH (32), so it is supported by a well-defined precedent. We were unable to detect oxaloacetate in any bacterial sample; thus, we cannot determine whether it accumulated in the cysteine deacetylase triple mutant (Δ*yxeP* Δ*sndAC*) as our proposed YxeK reaction schemes suggest it might (Fig. 5*D*). In any case, further biochemical studies are needed to elucidate how YxeK forms NAC from *N*-acetyl-2SC.

The last step in the pathway is deacetylation of NAC to give cysteine. Our results show that deacetylation can occur by YxeP or other functionally redundant NAC deacetylases (Figs. 3*B* and 5*C*). Growth assays indicate that *yxeM*, *yxeN*, and *yxeO*, which are predicted to encode the three subunits of an ABC-type transporter, are not essential for 2SC utilization in *B. subtilis* (Fig. 3*A*). Still, there is reason to suspect a 2SC transport function for these genes. Our Tn-seq results show that transposon insertions in these genes slightly decrease fitness when grown on 2SC-containing medium (Fig. 2). Furthermore, *B. subtilis* has at least one other ABC-type transporter that has been shown to transport sulfur-containing compounds, including *S*-alkyl-derivatives of cysteine (33–36). *yxeMNO* genes may encode a 2SC transporter that is not essential for growth on 2SC in *B. subtilis* because of functional redundancy. Similarly, *yxeQ* is not essential for 2SC utilization, but this could also be due to functional redundancy. It is also possible that *yxeQ* allows the *yxe* operon to participate in the disposal of compounds other than 2SC.

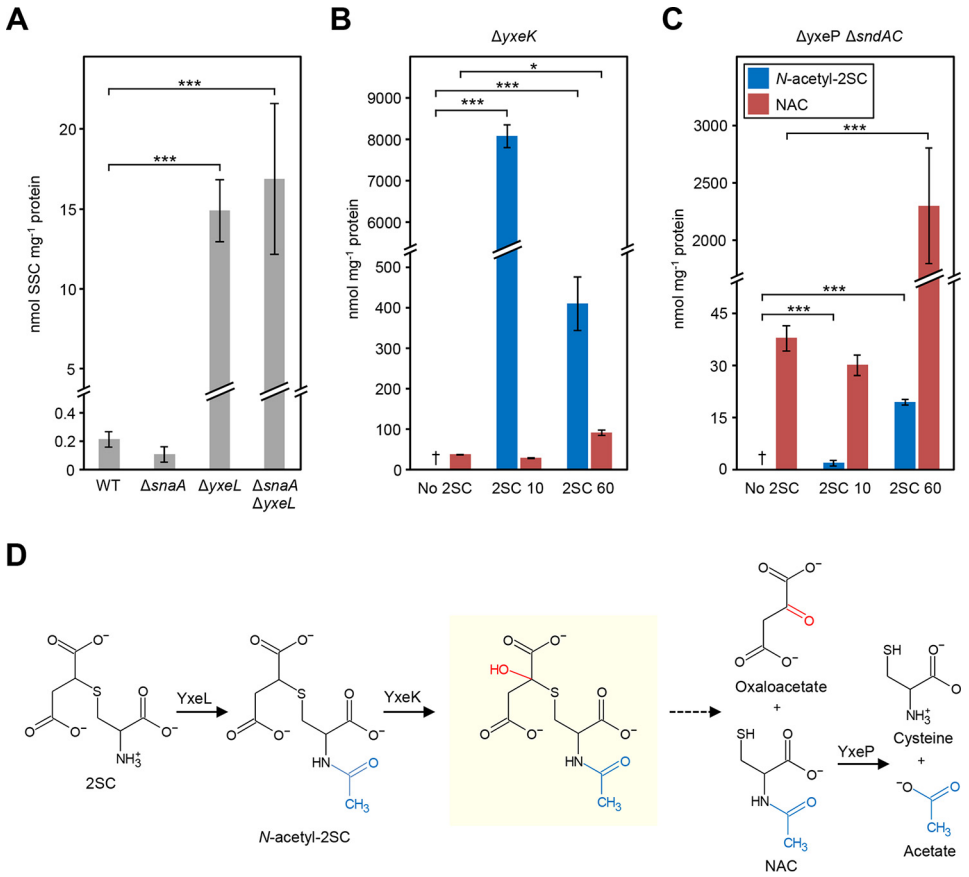

Figure 5. Accumulation of 2SC, *N*-acetyl-2SC, and NAC in various *B. subtilis* mutants supports a proposed breakdown pathway. *A*, accumulation of 2SC in WT *B. subtilis* and Δ*snaA*, Δ*yxeL*, and Δ*snaA*Δ*yxeL* mutant cells grown on minimal medium containing fumarate as the carbon source. *B* and *C*, accumulation of *N*-acetyl-2SC and NAC in Δ*yxeK* (*B*) and Δ*yxeP* Δ*sndAC* (*C*) cells grown on minimal medium containing glucose as the carbon source without (*No 2SC*) or with the addition of 2SC to 0.5 mM either 10 (*2SC 10*) or 60 min (*2SC 60*) before harvesting the cells. Data represent means and S.E. (*error bars*) of three replicates. *Asterisks* denote levels that are significantly different (*, $p < 0.05$; ***, $p < 0.001$; *t* test). †, not detectable (detection limit, 0.1 nmol mg^{-1} protein). *D*, proposed breakdown pathway for 2SC in *B. subtilis*. A possible reaction mechanism for YxeK as discussed in the text is shown. *Solid* or *dotted lines* indicate enzyme-catalyzed or spontaneous reactions, respectively.

The 2SC breakdown pathway involves acetylation, oxygenation-initiated deconstruction, and deacetylation, which is similar to the pathway proposed for the metabolism of *S*-methylcysteine, and the operons that are primarily used to metabolize each compound (the *yxe* operon and *ytmItcyJKLMNytmOytnIJrbfKytnLM* operon) are similar in content as noted previously (26). This is likely the reason for the high degree of functional redundancy observed between enzymes of each operon in the breakdown of 2SC and *S*-methylcysteine. The deacetylases (and probably ABC-type transporters) perform essentially the same task and can efficiently moonlight in the breakdown of either compound, whereas the acetyltransferases and monooxygenases perform more specialized tasks and have a limited ability to moonlight. Based on our evidence that the *yxe* operon is predominantly responsible for 2SC breakdown, we propose renaming it as the *S*-(2-succino)cysteine metabolism (*scm*) operon.

To our knowledge, this is the first demonstration of a metabolic route for 2SC breakdown. It was previously reported that succinated GSH is a substrate of GSH reductase (37). However, these results are almost certainly artifactual because (*a*) dimethyl fumarate was used instead of fumarate to succinate GSH, (*b*) a mixture of dimethyl fumarate and GSH was assayed instead of purified substrate, and (*c*) the reaction GSH reductase catalyzes, reduction of a disulfide bond, is different from the hydrolysis reaction needed to break the thioether bond of succinated GSH. Furthermore, we were unable to replicate this finding *in vitro* with GSH reductase enzyme assays. The expected enzyme activity was detected with GSH disulfide as a substrate, but we could not detect any activity with purified *S*-(2-succino)GSH, 2SC, or *N*-acetyl-2SC as substrates (Table S1).

Although it is well-established that succination of cellular thiols can have deleterious effects *in vivo* (*e.g.* by inactivating enzymes with functional cysteine residues (18–21)), this is the first report that 2SC itself is toxic, at least to *B. subtilis*. Breakdown of 2SC may be an important way to deal with this unavoidable and toxic product of metabolism, more so than as a means to recycle a damaged metabolite. Acetylation appears to be a common strategy for prokaryotes to manage toxic and/or reactive compounds. Bacteria often have specific acetyltransferases that prevent the toxic buildup of sugars such as lactose (38) and maltose (39, 40), and acetylation of antibiotics is a common mechanism of bacterial resistance (41). 2SC disposal substantiates the emerging paradigm that cells often handle toxic metabolites by pathways that begin with acetylation and end with deacetylation in direct analogy to the blocking–deblocking strategies used in organic chemistry (26).

The *yxe* operon occurs in widely taxonomically diverse bacteria (Fig. S3), but the total number of species containing this operon is quite small. Of a representative set of over 1600 diverse bacterial genomes (see "Experimental procedures"), the *yxe* operon (defined as containing the monooxygenase and at least two of the acetyltransferase, deacetylase, putative dehydratase, and ABC transporter subunits) occurs in only 21. Homologs of the monooxygenase gene *yxeK*, which is the most distinct gene in the pathway and perhaps an indicator for the ability to breakdown 2SC, are found outside of the context of the *yxe* operon but are still limited to Bacteria, Archaea, and Ascomycota fungi. Because succination of thiols is likely to occur nearly ubiquitously, this raises the possibility that other distinct 2SC breakdown pathways exist. It is also possible that most organisms do not metabolize 2SC but instead simply excrete it. If this were the case, then having a breakdown pathway would enable the utilization of 2SC that has been released to the environment.

Humans lack homologs of the *yxe* genes, and it is so far unknown whether they have a pathway to metabolize 2SC. Our work provides an example of how such a pathway could operate. Considering the importance of succination to the progression of diseases such as diabetes (15–17, 42) and, in general, of the role spontaneous modifications of macromolecules is thought to play in aging (43), the identification of a mammalian system to metabolize 2SC, or otherwise deal with 2SC accumulation, could provide important medical insights.

Experimental procedures

Bioinformatics

DNA and protein sequences were from GenBank™ or SEED (44). A representative set of 1641 bacterial and archaeal genomes was analyzed using SEED tools (44). The *yxe* operon consists of seven genes: *yxeK* (UniProt ID P54950), *yxeL* (UniProt ID P54951), *yxeMNO* (UniProt IDs P54952, P54953, and P54954), *yxeP* (UniProt ID P54955), and *yxeQ* (UniProt ID P54956).

Chemicals

2SC was made by combining 40 mmol of cysteine with 45 mmol of sodium fumarate in 50 ml of water, adjusting pH to 8.0 with NaOH, and incubating at 22 °C for 35 h with stirring. The mixture was lyophilized, and the resulting crystals were stored at −20 °C. 2SC was further purified by HPLC using a Hypersil GOLD 250 × 4.6-mm C_{18} column (Fisher Scientific) with 0.1% formic acid as the mobile phase (flow rate, 1.0 ml min^{-1}). Fractions containing 2SC (detected by absorbance at 210 nm) were collected, and successive runs were pooled, lyophilized, and stored at −20 °C. *S*-(2-Succino)GSH and *N*-acetyl-2SC were synthesized and purified in the same manner except that 8 mmol of GSH and 9 mmol of sodium fumarate were combined in 15 ml of water or 8 mmol of *N*-acetyl-L-cysteine and 9 mmol of sodium fumarate were combined in 12 ml of water, respectively. All other chemicals were from Sigma-Aldrich.

Bacterial strains and culture conditions

All strains are listed in Table S2. All BKE mutant loci were back-crossed into WT *B. subtilis* 168 by transforming 5 μg of isolated DNA into WT cells (45) and selecting for recombinants on LB agar plates containing 1 μg ml^{-1} erythromycin and 25 μg ml^{-1} lincomycin. The presence of the BKE cassette in the expected locus was verified (Fig. S5). The *B. subtilis* transposon library used for Tn-seq experiments was described previously (25). For growth assays and preparing Tn-seq and metabolite profiling samples, strains were grown in ED minimal medium (8 mM K_2HPO_4, 4.4 mM KH_2PO_4, 30 mM NH_4Cl, 2 mM $MgSO_4$, 0.6 mM $MgCl_2$, 27 mM glucose, 0.3 mM Na_3-citrate, 0.25 mM L-tryptophan, 0.1 mM $FeCl_3$, 50 μM $CaCl_2$, 5 μM $MnCl_2$, 12 μM $ZnCl_2$, 2.5 μM $CuCl_2$, 2.5 μM $CoCl_2$, and 2.5 μM Na_2MoO_4). To prepare medium with 1 mM 2SC or methionine as the sulfur source (or for medium with no sulfur), $MgSO_4$ was replaced with $MgCl_2$ at the same magnesium concentration (2 mM). Solid medium was prepared by adding low-melt agarose to a final concentration of 0.8% (w/v). Growth assays were performed as indicated. To prepare samples for Tn-seq, 0.4 ml of the *B. subtilis* transposon library (stored at −80 °C at an optical density (600 nm) of 1.0) was combined with 7.6 ml of LB medium and incubated at 37 °C with shaking for 1.5 h until optical density reached 0.38. The library was then washed twice in ED minimal medium (without sulfur) and used to inoculate 20 ml of ED medium or ED medium containing either 2 mM sulfate, 1 mM Met, or 1 mM 2SC to an optical density of 0.02. Cultures were incubated at 37 °C with shaking for 9–10 h until optical density reached 1.3 (six doublings) at which point the cells were harvested by centrifugation (8000 × *g*, 10 min), frozen in liquid N_2, and stored at −80 °C. For preparing metabolite profiling samples, glucose was replaced with 30 mM sodium fumarate (when indicated). Overnight cultures were used to inoculate fresh medium to an optical density of 0.05, and cultures were grown at 37 °C with shaking for 6–8 h until optical density reached 1.5 ± 0.1 at which point an equivalent of 2 ml at optical density of 1.0 was harvested by centrifugation (21,000 × *g*, 30 s), frozen in liquid N_2, and stored at −80 °C. When indicated, 2SC was added to a final concentration of 0.5 mM either 10 min or 1 h before harvesting.

Tn-seq analysis

Tn-seq was performed essentially as described previously (25, 46). DNA was isolated from the harvested cell pellets using the GeneJET Genomic DNA Purification kit (Thermo Scientific, Waltham, MA). 6 μg of DNA was treated with the restriction enzyme MmeI (New England Biolabs, Ipswich, MA) for 3 h at 37 °C, then 10 units of calf intestine phosphatase (New England Biolabs) was added, and incubation was continued for 1 h. The DNA was then extracted and precipitated (25) and dissolved in 27.5 μl of 2 mM Tris-Cl, pH 8.5. To the DNA was added 2 μl of annealed DNA adapter (200 mM each of oCJ25 and oCJ26 oligonucleotides prepared as described (25)), 3.5 μl of 10× T4 DNA ligase buffer, and 1.5 μl (600 units) of T4 DNA ligase (New England Biolabs). The ligation mixture was incubated for 16 h at 16 °C, and DNA was isolated with the GeneJET Genomic DNA Purification kit. 5 μl of adapter-ligated DNA was used in PCRs with the oCJ23 primer and either primer oCJ22-2 (sulfate-grown sample), oCJ22-4 (methionine-grown sample), or oCJ22-6 (2SC-grown sample) as described previously (25). PCR products were electrophoresed on 2% agarose

gels, the ~128-bp band of interest was excised, and the DNA was recovered in 15 μl of 10 mM Tris-Cl, pH 8.5, with a DNA Gel Extraction Mini kit (Qiagen, Hilden, Germany). Sequencing was performed at the University of Florida NextGen DNA Sequencing facility (University of Florida Interdisciplinary Center for Biotechnology Research). Using the oCJ24 oligonucleotide to obtain the primary sequence and oCJ27 oligonucleotide to obtain the barcode sequences, we first used a MiSeq system (Illumina, San Diego, CA) for 1 × 50 cycles to determine how much to load for optimum clustering. Sequencing was then performed for 50 cycles with a NextSeq 500 (Illumina) using a 1 × 75 high-throughput v2 cartridge. Custom primers (25) were added to the standard Illumina primers to allow for use of PhiX (10%). Approximately 320 million "passing-filter" reads were generated per run. The data were trimmed with Illumina software to remove everything except the 16–17-bp region corresponding to the transposon–genome junctions. Transposon insertion sites were mapped in the *B. subtilis* reference genome sequence (NC_000964.3) using 16-mer sequence tags. *k*-mer profiles (16-mer) were generated for sequence data sets from each of the three treatments, SO_4, Met, and 2SC, using the count function of JELLYFISH (47). The *k*-mer count profiles were then queried with the reference genome sequence using the query function of JELLYFISH to determine relative frequencies and genome coordinates of insertions for each treatment. Insertion coordinates were then overlaid with the genome annotation (AL009126.gff) to identify genes that were differentially targeted in the three data sets.

E. coli expression constructs

All constructs were sequence-verified. Full-length cDNAs for *B. subtilis* YxeL (UniProt ID P54951) and SnaA (UniProt ID O34350) were PCR-amplified from genomic DNA of *B. subtilis* strain 168 with Phusion High-Fidelity DNA polymerase (New England Biolabs) using primer pair 5′-ggaattccatatgaagccacgataccgccttgc-3′ and 5′-ggaattcttatagatcatgtcgcaattgttt-3′ and primer pair 5′-ggaattccatatgagtgatgatatttttcgactggc-3′ and 5′-ggaattctcatgcccagctgggcgcac-3′, respectively. The amplified DNAs were digested with NdeI/EcoRI and ligated into the matching sites of pET28b (Novagen), which added an N-terminal His_6 tag.

Production and purification of proteins

The pET28b plasmids containing the *snaA* or *yxeL* coding sequences were transformed into BL21-(DE3)-RIPL (Stratagene) cells. Cultures (100 ml) were grown at 37 °C in LB medium containing 50 μg/ml kanamycin. When optical density reached 0.8, isopropyl β-D-thiogalactoside was added (final concentration, 0.5 mM), and incubation was continued for 3 h at 37 °C. Cells were harvested by centrifugation (8000 × *g*, 10 min); resuspended in 5 ml of 50 mM potassium phosphate, pH 8.0, 300 mM NaCl, and 10 mM imidazole; and sonicated (Fisher Scientific Ultrasonic Dismembrator, model 150E) for 5 × 15-s pulses at 70% power, cooling on ice for 60 s between pulses. The lysate was centrifuged at 17,000 × *g* for 10 min, and the supernatant was added to a column containing 0.25 ml of Ni^{2+}-nitrilotriacetic acid resin (Qiagen). After washing with 25 ml of 50 mM potassium phosphate, pH 8.0, 300 mM NaCl, and 20 mM imidazole, proteins were eluted with 0.5 ml of this buffer containing 250 mM imidazole and desalted on PD-10 columns (GE Healthcare) equilibrated in 50 mM Tris-HCl, pH 8.0, 100 mM KCl, 10% (v/v) glycerol. Proteins were concentrated to 3.5–8.0 mg ml^{-1} with Amicon Ultra-4 10,000 units (Millipore), then aliquoted, frozen in liquid N_2, and stored at −80 °C.

Enzyme assays

Purified SnaA and SnaB proteins were assayed for acetyltransferase activity against 2SC using Ellman's reagent as described previously (48, 49). Assays (50-μl total volume) contained 50 mM Tris-Cl, pH 7.5, 0.4 mM acetyl-CoA, and between 8.0 and 0.001 mM 2SC and were started by adding either 8.8 μg of SnaA or 4.0 ng of SnaB. After a 10-min incubation at 37 °C, 50 μl of a solution containing 50 mM Tris-Cl, pH 7.5, and 6 M guanidine HCl was added to stop the reaction. 50 μl of Ellman's reagent (50 mM Tris-Cl, pH 7.5, 0.2 mM 5,5′-dithiobis(2-nitrobenzoic acid), and 1 mM EDTA) was added, and the mixture was incubated at 22 °C for 10 min before measuring optical density at 412 nm. Assays were replicated at least three times. An extinction coefficient of 14,150 cm^{-1} M^{-1} for 3-carboxy-4-nitrobenzenethiol was used to calculate the amount of CoA formed. Kinetic parameters were calculated by fitting data to the Michaelis–Menten equation using GraphPad Prism Software (version 4.00 for Windows, GraphPad Software, San Diego, CA).

Metabolic profiling

Extractions were performed essentially as described (50). Briefly, 0.5 ml of ice-cold 80:20 (v/v) acetonitrile/water was added to each sample and shaken at 4 °C for 15 min on an orbital shaker (Torrey Pines Scientific) at maximum speed and centrifuged at 14,000 × *g*, and 0.5 ml of supernatant was transferred to a clean microcentrifuge tube. The extraction process was repeated to give a total cell extract volume of 1 ml. Aliquots (0.2 ml) of the cell extract were dried under vacuum at room temperature and frozen at −20 °C. For metabolic profiling, samples were resuspended in 0.05 ml of acetonitrile/water (4:1, v/v) containing internal standards (*e.g.* 5 μg/ml Val-Tyr-Val). 5 μl was injected onto a hydrophobic interaction LC column (Waters Acquity UPLC BEH Amide, 150-mm length × 2.1-mm inner diameter, 1.7-μm particle size) with guard column (Acquity VanGuard BEH Amide precolumn, 5-mm length × 2.1-mm inner diameter, 1.7-μm particle size) held at 45 °C on a Thermo Fisher Vanquish Focused ultra HPLC system. Mobile phase A was LC-MS–grade water with 10 mM ammonium formate and 0.125% formic acid. Mobile phase B was LC-MS–grade 95:5 (v/v) acetonitrile/water with 10 mM ammonium formate and 0.125% formic acid. Total run time per sample was 17 min with a flow rate of 0.4 ml/min. The gradient started at 100% B for 2 min; was brought to 70% B by 7.7 min, 40% B by 9.5 min, and back to 100% B by 12.75 min; and then was held at 100% B until 17 min. Mass spectra were recorded on a Thermo Fisher Q-Exactive HF mass spectrometer in positive mode between 60 and 900 *m*/*z*. Data were collected at resolutions of 60,000 for MS1 and 15,000 for MS/MS. MS/MS information was collected under data-dependent conditions for the top four ions per MS1 scan with one *m*/*z* isolation window and normalized collision

energy of 20, 30, and 40. Automatic gain control target was set at one million ions for MS1 and 150,000 ions for MS/MS. Capillary temperature was set to 300 °C, spray voltage was 3 kV, and auxiliary gas flow rate was set to 20. *S*-(2-Succino)cysteine, *N*-acetyl-2SC, and *N*-acetylcysteine standards were used to identify and quantify these metabolites based on accurate mass, retention time, and MS/MS matching. Peak height was used for quantification. For each standard, an MS/MS spectrum was uploaded to the Mass Bank of North America (MONA) database. Open source software MS-DIAL (51) was used for peak deconvolution, peak picking, alignment, and MS/MS matching.

Author contributions—T. D. N. and A. D. H. conceptualization; T. D. N., J. F., D. R. M., and D. M. A. data curation; T. D. N., J. F., and O. F. investigation; T. D. N. and A. J. L. C. writing-original draft; T. D. N. and A. D. H. writing-review and editing.

Acknowledgments—We thank Christopher M. Johnson for providing the B. subtilis transposon library and for advice related to Tn-seq. We thank Antoine Danchin, Daniel Ziegler and the Bacillus Genetic Stock Center for providing B. subtilis strains and for advice. We thank Valérie de Crécy-Lagard and Leticia Pollo de Oliveira for advice.

References

1. Schmidt, T. J., Ak, M., and Mrowietz, U. (2007) Reactivity of dimethyl fumarate and methylhydrogen fumarate towards glutathione and N-acetyl-L-cysteine—preparation of S-substituted thiosuccinic acid esters. *Bioorg. Med. Chem.* **15,** 333–342
2. Alderson, N. L., Wang, Y., Blatnik, M., Frizzell, N., Walla, M. D., Lyons, T. J., Alt, N., Carson, J. A., Nagai, R., Thorpe, S. R., and Baynes, J. W. (2006) S-(2-Succinyl)cysteine: a novel chemical modification of tissue proteins by a Krebs cycle intermediate. *Arch. Biochem. Biophys.* **450,** 1–8 CrossRef Medline
3. Thorpe, S. R., and Baynes, J. W. (2003) Maillard reaction products in tissue proteins: new products and new perspectives. *Amino Acids* **25,** 275–281 CrossRef Medline
4. Nagai, R., Brock, J. W., Blatnik, M., Baatz, J. E., Bethard, J., Walla, M. D., Thorpe, S. R., Baynes, J. W., and Frizzell, N. (2007) Succination of protein thiols during adipocyte maturation: a biomarker of mitochondrial stress. *J. Biol. Chem.* **282,** 34219–34228 CrossRef Medline
5. Blatnik, M., Frizzell, N., Thorpe, S. R., and Baynes, J. W. (2008) Inactivation of glyceraldehyde-3-phosphate dehydrogenase by fumarate in diabetes: formation of S-(2-succinyl)cysteine, a novel chemical modification of protein and possible biomarker of mitochondrial stress. *Diabetes* **57,** 41–49 CrossRef Medline
6. Blatnik, M., Thorpe, S. R., and Baynes, J. W. (2008) Succination of proteins by fumarate: mechanism of inactivation of glyceraldehyde-3-phosphate dehydrogenase in diabetes. *Ann. N.Y. Acad. Sci.* **1126,** 272–275 CrossRef Medline
7. Ternette, N., Yang, M., Laroyia, M., Kitagawa, M., O'Flaherty, L., Wolhulter, K., Igarashi, K., Saito, K., Kato, K., Fischer, R., Berquand, A., Kessler, B. M., Lappin, T., Frizzell, N., Soga, T., *et al.* (2013) Inhibition of mitochondrial aconitase by succination in fumarate hydratase deficiency. *Cell Rep.* **3,** 689–700 CrossRef Medline
8. Piroli, G. G., Manuel, A. M., Walla, M. D., Jepson, M. J., Brock, J. W., Rajesh, M. P., Tanis, R. M., Cotham, W. E., and Frizzell, N. (2014) Identification of protein succination as a novel modification of tubulin. *Biochem. J.* **462,** 231–245 CrossRef Medline
9. Frizzell, N., Lima, M., and Baynes, J. W. (2011) Succination of proteins in diabetes. *Free Radic. Res.* **45,** 101–109 CrossRef Medline
10. Miglio, G., Sabatino, A. D., Veglia, E., Giraudo, M. T., Beccuti, M., and Cordero, F. (2016) A computational analysis of S-(2-succino)cysteine sites in proteins. *Biochim. Biophys. Acta* **1864,** 211–218 CrossRef Medline
11. Bardella, C., El-Bahrawy, M., Frizzell, N., Adam, J., Ternette, N., Hatipoglu, E., Howarth, K., O'Flaherty, L., Roberts, I., Turner, G., Taylor, J., Giaslakiotis, K., Macaulay, V. M., Harris, A. L., Chandra, A., *et al.* (2011) Aberrant succination of proteins in fumarate hydratase-deficient mice and HLRCC patients is a robust biomarker of mutation status. *J. Pathol.* **225,** 4–11 CrossRef Medline
12. Adam, J., Hatipoglu, E., O'Flaherty, L., Ternette, N., Sahgal, N., Lockstone, H., Baban, D., Nye, E., Stamp, G. W., Wolhuter, K., Stevens, M., Fischer, R., Carmeliet, P., Maxwell, P. H., Pugh, C. W., *et al.* (2011) Renal cyst formation in Fh1-deficient mice is independent of the Hif/Phd pathway: roles for fumarate in KEAP1 succination and Nrf2 signaling. *Cancer Cell* **20,** 524–537 CrossRef Medline
13. Reyes, C., Karamurzin, Y., Frizzell, N., Garg, K., Nonaka, D., Chen, Y. B., and Soslow, R. A. (2014) Uterine smooth muscle tumors with features suggesting fumarate hydratase aberration: detailed morphologic analysis and correlation with S-(2-succino)-cysteine immunohistochemistry. *Mod. Pathol.* **27,** 1020–1027 CrossRef Medline
14. Yang, M., Soga, T., and Pollard, P. J. (2013) Oncometabolites: linking altered metabolism with cancer. *J. Clin. Investig.* **123,** 3652–3658 CrossRef Medline
15. Frizzell, N., Rajesh, M., Jepson, M. J., Nagai, R., Carson, J. A., Thorpe, S. R., and Baynes, J. W. (2009) Succination of thiol groups in adipose tissue proteins in diabetes: succination inhibits polymerization and secretion of adiponectin. *J. Biol. Chem.* **284,** 25772–25781 CrossRef Medline
16. Thomas, S. A., Storey, K. B., Baynes, J. W., and Frizzell, N. (2012) Tissue distribution of S-(2-succino)cysteine (2SC), a biomarker of mitochondrial stress in obesity and diabetes. *Obesity* **20,** 263–269 CrossRef Medline
17. Frizzell, N., Thomas, S. A., Carson, J. A., and Baynes, J. W. (2012) Mitochondrial stress causes increased succination of proteins in adipocytes in response to glucotoxicity. *Biochem. J.* **445,** 247–254 CrossRef Medline
18. Merkley, E. D., Metz, T. O., Smith, R. D., Baynes, J. W., and Frizzell, N. (2014) The succinated proteome. *Mass Spectrom. Rev.* **33,** 98–109 CrossRef Medline
19. Hoekstra, A. S., de Graaff, M. A., Briaire-de Bruijn, I. H., Ras, C., Seifar, R. M., van Minderhout, I., Cornelisse, C. J., Hogendoorn, P. C., Breuning, M. H., Suijker, J., Korpershoek, E., Kunst, H. P., Frizzell, N., Devilee, P., Bayley, J. P., *et al.* (2015) Inactivation of SDH and FH cause loss of 5hmC and increased H3K9me3 in paraganglioma/pheochromocytoma and smooth muscle tumors. *Oncotarget* **6,** 38777–38788 CrossRef Medline
20. Piroli, G. G., Manuel, A. M., Clapper, A. C., Walla, M. D., Baatz, J. E., Palmiter, R. D., Quintana, A., and Frizzell, N. (2016) Succination is increased on select proteins in the brainstem of the NADH dehydrogenase (ubiquinone) Fe-S protein 4 (Ndufs4) knockout mouse, a model of Leigh syndrome. *Mol. Cell. Proteomics* **15,** 445–461 CrossRef Medline
21. Ruecker, N., Jansen, R., Trujillo, C., Puckett, S., Jayachandran, P., Piroli, G. G., Frizzell, N., Molina, H., Rhee, K. Y., and Ehrt, S. (2017) Fumarase deficiency causes protein and metabolite succination and intoxicates *Mycobacterium tuberculosis*. *Cell Chem. Biol.* **24,** 306–315 CrossRef Medline
22. Zheng, L., Cardaci, S., Jerby, L., MacKenzie, E. D., Sciacovelli, M., Johnson, T. I., Gaude, E., King, A., Leach, J. D., Edrada-Ebel, R., Hedley, A., Morrice, N. A., Kalna, G., Blyth, K., Ruppin, E., *et al.* (2015) Fumarate induces redox-dependent senescence by modifying glutathione metabolism. *Nat. Commun.* **6,** 6001 CrossRef Medline
23. Manuel, A. M., Walla, M. D., Faccenda, A., Martin, S. L., Tanis, R. M., Piroli, G. G., Adam, J., Kantor, B., Mutus, B., Townsend, D. M., and Frizzell, N. (2017) Succination of protein disulfide isomerase links mitochondrial stress and endoplasmic reticulum stress in the adipocyte during diabetes. *Antioxid. Redox Signal.* **27,** 1281–1296 CrossRef Medline
24. Hullo, M. F., Auger, S., Soutourina, O., Barzu, O., Yvon, M., Danchin, A., and Martin-Verstraete, I. (2007) Conversion of methionine to cysteine in *Bacillus subtilis* and its regulation. *J. Bacteriol.* **189,** 187–197 CrossRef Medline
25. Johnson, C. M., and Grossman, A. D. (2014) Identification of host genes that affect acquisition of an integrative and conjugative element in *Bacillus subtilis*. *Mol. Microbiol.* **93,** 1284–1301 CrossRef Medline
26. Chan, C. M., Danchin, A., Marlière, P., and Sekowska, A. (2014) Paralogous metabolism: S-alkyl-cysteine degradation in *Bacillus subtilis*. *Environ. Microbiol.* **16,** 101–117 CrossRef Medline

27. Koo, B. M., Kritikos, G., Farelli, J. D., Todor, H., Tong, K., Kimsey, H., Wapinski, I., Galardini, M., Cabal, A., Peters, J. M., Hachmann, A. B., Rudner, D. Z., Allen, K. N., Typas, A., and Gross, C. A. (2017) Construction and analysis of two genome-scale deletion libraries for *Bacillus subtilis*. *Cell Syst.* **4,** 291–305.e7 CrossRef Medline
28. Limsuwun, K., and Jones, P. G. (2000) Spermidine acetyltransferase is required to prevent spermidine toxicity at low temperatures in *Escherichia coli*. *J. Bacteriol.* **182,** 5373–5380 CrossRef Medline
29. Oda, K., Matoba, Y., Kumagai, T., Noda, M., and Sugiyama, M. (2013) Crystallographic study to determine the substrate specificity of an L-serine-acetylating enzyme found in the D-cycloserine biosynthetic pathway. *J. Bacteriol.* **195,** 1741–1749 CrossRef Medline
30. Yu, A. C., Loo, J. F., Yu, S., Kong, S. K., and Chan, T. F. (2014) Monitoring bacterial growth using tunable resistive pulse sensing with a pore-based technique. *Appl. Microbiol. Biotechnol.* **98,** 855–862 CrossRef Medline
31. Linster, C. L., Van Schaftingen, E., and Hanson, A. D. (2013) Metabolite damage and its repair or pre-emption. *Nat. Chem. Biol.* **9,** 72–80 CrossRef Medline
32. Thornalley, P. J. (2003) Glyoxalase I—structure, function and a critical role in the enzymatic defence against glycation. *Biochem. Soc. Trans.* **31,** 1343–1348 CrossRef Medline
33. van der Ploeg, J. R., Cummings, N. J., Leisinger, T., and Connerton, I. F. (1998) *Bacillus subtilis* genes for the utilization of sulfur from aliphatic sulfonates. *Microbiology* **144,** 2555–2561 CrossRef Medline
34. Sekowska, A., Robin, S., Daudin, J. J., Hénaut, A., and Danchin, A. (2001) Extracting biological information from DNA arrays: an unexpected link between arginine and methionine metabolism in *Bacillus subtilis*. *Genome Biol.* **2,** RESEARCH0019 Medline
35. Burguière, P., Fert, J., Guillouard, I., Auger, S., Danchin, A., and Martin-Verstraete, I. (2005) Regulation of the *Bacillus subtilis* ytmI operon, involved in sulfur metabolism. *J. Bacteriol.* **187,** 6019–6030 CrossRef Medline
36. Higashitsuji, Y., Angerer, A., Berghaus, S., Hobl, B., and Mack, M. (2007) RibR, a possible regulator of the *Bacillus subtilis* riboflavin biosynthetic operon, *in vivo* interacts with the 5′-untranslated leader of rib mRNA. *FEMS Microbiol. Lett.* **274,** 48–54 CrossRef Medline
37. Sullivan, L. B., Martinez-Garcia, E., Nguyen, H., Mullen, A. R., Dufour, E., Sudarshan, S., Licht, J. D., Deberardinis, R. J., and Chandel, N. S. (2013) The proto-oncometabolite fumarate binds glutathione to amplify ROS-dependent signaling. *Mol. Cell* **51,** 236–248 CrossRef Medline
38. Danchin, A. (2009) Cells need safety valves. *Bioessays* **31,** 769–773 CrossRef Medline
39. Brand, B., and Boos, W. (1991) Maltose transacetylase of *Escherichia coli*. Mapping and cloning of its structural, gene, mac, and characterization of the enzyme as a dimer of identical polypeptides with a molecular weight of 20,000. *J. Biol. Chem.* **266,** 14113–14118 Medline
40. Dippel, R., and Boos, W. (2005) The maltodextrin system of *Escherichia coli*: metabolism and transport. *J. Bacteriol.* **187,** 8322–8331 CrossRef Medline
41. Wright, G. D. (2005) Bacterial resistance to antibiotics: enzymatic degradation and modification. *Adv. Drug Deliv. Rev.* **57,** 1451–1470 CrossRef Medline
42. Adam, J., Ramracheya, R., Chibalina, M. V., Ternette, N., Hamilton, A., Tarasov, A. I., Zhang, Q., Rebelato, E., Rorsman, N. J. G., Martín-Del-Río, R., Lewis, A., Özkan, G., Do, H. W., Spégel, P., Saitoh, K., *et al.* (2017) Fumarate hydratase deletion in pancreatic β cells leads to progressive diabetes. *Cell Rep.* **20,** 3135–3148 CrossRef Medline
43. Gladyshev, V. N. (2014) The free radical theory of aging is dead. Long live the damage theory! *Antioxid. Redox Signal.* **20,** 727–731 CrossRef Medline
44. Overbeek, R., Begley, T., Butler, R. M., Choudhuri, J. V.., Chuang, H. Y., Cohoon, M., de Crécy-Lagard, V., Diaz, N., Disz, T., Edwards, R., Fonstein, M., Frank, E. D., Gerdes, S., Glass, E. M., Goesmann, A., *et al.* (2005) The subsystems approach to genome annotation and its use in the project to annotate 1000 genomes. *Nucleic Acids Res.* **33,** 5691–5702 CrossRef Medline
45. Niehaus, T. D., Elbadawi-Sidhu, M., de Crécy-Lagard, V., Fiehn, O., and Hanson, A. D. (2017) Discovery of a widespread prokaryotic 5-oxoprolinase that was hiding in plain sight. *J. Biol. Chem.* **292,** 16360–16367 CrossRef Medline
46. van Opijnen, T., Lazinski, D. W., and Camilli, A. (2015) Genome-wide fitness and genetic interactions determined by Tn-seq, a high-throughput massively parallel sequencing method for microorganisms. *Curr. Protoc. Microbiol.* **36,** 1E.3.1–1E.3.24 CrossRef Medline
47. Marçais, G., and Kingsford, C. (2011) A fast, lock-free approach for efficient parallel counting of occurrences of *k*-mers. *Bioinformatics* **27,** 764–770 CrossRef Medline
48. Lin, H. J., Lien, Y. C., and Hsu, C. H. (2010) A high-throughput colorimetric assay to characterize the enzyme kinetic and cellular activity of spermidine/spermine N1-acetyltransferase 1. *Anal. Biochem.* **407,** 226–232 CrossRef Medline
49. Qiu, J., Wang, D., Ma, Y., Jiang, T., and Xin, Y. (2013) Identification and characterization of serine acetyltransferase encoded by the *Mycobacterium tuberculosis* Rv2335 gene. *Int. J. Mol. Med.***31,** 1229–1233 CrossRef Medline
50. Rabinowitz, J. D., and Kimball, E. (2007) Acidic acetonitrile for cellular metabolome extraction from *Escherichia coli*. *Anal. Chem.* **79,** 6167–6173 CrossRef Medline
51. Tsugawa, H., Cajka, T., Kind, T., Ma, Y., Higgins, B., Ikeda, K., Kanazawa, M., VanderGheynst, J., Fiehn, O., and Arita, M. (2015) MS-DIAL: data-independent MS/MS deconvolution for comprehensive metabolome analysis. *Nat. Methods* **12,** 523–526 CrossRef Medline